Experimental Investigation of Rotational Control of a Constrained Quadrotor Using Backstepping Method

N.Parhizkar*, A.Naghash†, and M.Naghshineh‡
Amirkabir University of technology

ABSTRACT

Considering nonlinear and simple dynamics of quadrotors, it is feasible to implement different types of control methods, so it is an appropriate subject for experimental research. In recent years, many researchers have investigated different aspects of quadrotors. In this study, at first, the utilized quad rotor is introduced and then its dynamics is modeled. Next step is to measure physical parameters of the quadrotor that are needed for simulation. Then, PID and Backstepping controllers are implemented in Simulink and after fixing translational motion of the quadrotor, both controllers are implemented on real model using Labview. Due to having 3DOF and 4 control inputs, the system is over-actuated, so an optimization is done to make the total thrust minimum. Results show that Euler angles are controlled by both PID and Backstepping controllers. Backstepping method has had better results.

1 INTRODUCTION

Many methods have been used for controlling quadrotors. Lyapunov theory has been used in [1],[2] for making sure to have asymptotic stability of system. PD and PID controllers have been used in many projects, for example in [3]. The advantage of PD and PID controllers is their easy implementation. PD and PID help us control a plant adequately without having full information of the plant characteristics or transfer functions. Adaptive techniques are used in [4] due to its good performance in cases of unmodeled dynamic and uncertainty. Classic LQR and SDRE (State-dependent Ricatti Equation) control are applied due to their advantage in presenting input signal from the feedback of the variables,[5],[6]. But the problem with this method is the difficulty of solution of the Ricatti equation. Backstepping Controller is another method that guarantees convergence of the inner variables but its calculations are complicated [7],[8]. Sliding mode controller is applied in much research and it is similar to backstepping method. This controller is robust to uncertainty in parameters and perturbations. The problem with this method is vibrations and chattering [9]. Other methods like dynamic feedback [10],visual feedback [11],Neural Networks [12] are used too but not as frequently as previously mentioned methods.

*M.S. graduate, parhizkar@aut.ac.ir
†Associate Professor, naghash@aut.ac.ir
‡PhD candidate, m.naghshineh@aut.ac.ir

2 AR. DRONE

The used quadrotor in this project is AR. Drone (Figure 1). AR. Drone is equipped with an inertial measurement unit (IMU) that measures pitch, roll, yaw and accelerations along all axes. The vehicle is controlled by sending commands over a Wi-Fi connection[13]. The AR. Drone carries an internal computer with a 468MHz ARM9-processor and 128MB of RAM, running a custom Linux operating system[13].

Figure 1: AR. Drone.

2.1 Gear Ratio

The gear ratio is defined as the input speed relative to the output speed. To obtain the gear ratio for the motor, it is enough to devide the number of teeth of the gear wheel for the motor to the gear wheel connected to the propeller. Two gear wheels have been shown in Figure 2. The gear ratio shown by G is as follows:

$$G = \frac{\text{motor gear wheel's teeth}}{\text{propeller gear wheel's teeth}} = \frac{69}{8} = 8.6 \quad (1)$$

Figure 2: The motor's and the propeller's gear wheels.

http://www.imavs.org/

http://www.imavs.org/

2.2 *Command to the motors*

AR.Drone has the capability to command its motors one by one directly using a parameter that it is shown by "n". This parameter can be changed from 0 to 500. It should be at least 5 to keep the motor running and the rotor speed will saturate for n=500. For simulation, it is necessary to know the relation between n and fm (the frequency of the motor signal). Different values of n are given to one of the motors and the motor voltage is observed in an oscilloscope. Then frequencies for different values of n are obtained. Figure3 indicates the voltage signal for n=10.

$$\omega_P = \frac{2\pi f_m}{G} \tag{2}$$

f_m is the frequency of the signal of the motor voltage and G is the gear ratio. Results have been shown in Figure 4.

$$(5 \leq n \leq 500) \qquad \omega_P = 0.724n + 125.9 \tag{3}$$

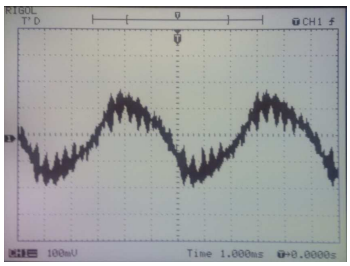

Figure 3: The signal of the motor voltage in n=10.

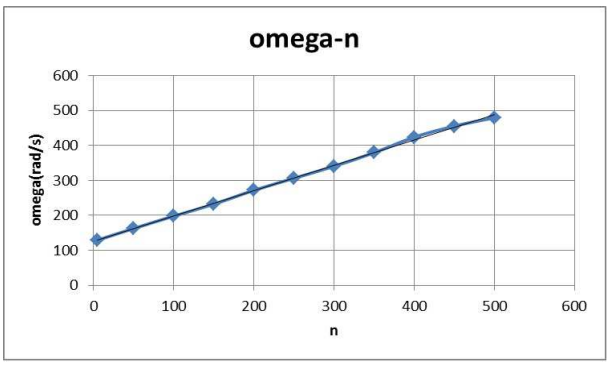

Figure 4: omegap versus different values of n.

3 ROTATIONAL DYNAMIC MODEL OF THE QUADROTOR

Dynamic model of the quadrotor is derived in [14] , [15] and it is just briefly explained. To develop dynamic model, it is assumed:

a. The structure and propellers are supposed to be rigid.

b. The structure is symmetrical and the body fixed frame origin is located on CG. The center of mass and the body fixed frame origin are assumed to coincide.

c. Propeller's thrust and drag are proportional to the square of its rotational speed.

d. Body drag due to motion and rotation is neglected due to low movement speed.

e. Ground effects are neglected and the earth is flat and fixed. Let us consider an inertial frame and a body fixed frame whose origin is in the center of mass of the quadrotor as shown in Figure 5.

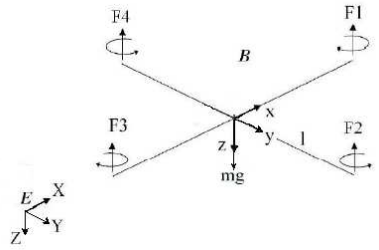

Figure 5: Body and Inertial Frames.

The orientation of the quadrotor is given by 3 Euler angles, namely yaw angle ψ, pitch angle θ and roll angle φ that together form the vector $[\varphi\ \theta\ \psi]^T$. To derive the equations of the rotational motion, Newton-Euler's formula is defined as following:

$$\vec{M} = \left.\frac{d(\vec{H})}{dt}\right)_{\substack{inertial\\frame}} = \left.\frac{d(\vec{H})}{dt}\right)_{\substack{Body\\frame}} + \vec{\omega} \times \vec{H} \tag{4}$$

$\vec{M}$ is the total external torque acting on the vehicle and $\vec{H}$ is the angular momentum made of one generated by body rotation and the other generated by the propeller's angular velocity:

$$\begin{aligned} \vec{H}_{body} &= \begin{bmatrix} I_x & 0 & 0 \\ 0 & I_y & 0 \\ 0 & 0 & I_z \end{bmatrix} . \begin{bmatrix} \omega_x \\ \omega_y \\ \omega_z \end{bmatrix} \quad , \\ \vec{H}_{blade} &= \begin{bmatrix} 0 \\ 0 \\ J_r \Omega_{blade} \end{bmatrix} \end{aligned} \tag{5}$$

Ω_{blade} is the difference between clockwise and counterclockwise propeller's angular velocity:

$$\Omega_{blade} = \Omega_1 + \Omega_3 - \Omega_2 - \Omega_4 \tag{6}$$

Ω_i , $i = 1, 2, 3, 4$, is the angular velocity of the each propeller. I_x, I_y and I_z are the moments of inertia and because of body symmetry, the products of inertia become zero. The

http://www.imavs.org/

following expression is used to obtain equation in inertial coordinate system:

$$\vec{M} = \begin{bmatrix} I_x\dot{\omega}_x + \omega_y\omega_z(I_z - I_y) + J_r\Omega\omega_y \\ I_y\dot{\omega}_y + \omega_x\omega_z(I_x - I_z) - J_r\Omega\omega_x \\ I_z\dot{\omega}_z + \omega_x\omega_y(I_y - I_x) \end{bmatrix} \quad (7)$$

$\vec{M}$ is moment's differences caused by angular velocity of the propeller. τ_i is the torque generated in the opposite direction of propeller rotation and is exerted on the propeller by air. For τ_i and T_i (thrust of motors), $i = 1, 2, 3, 4$, we have:

$$\tau_i = d\Omega_i^2 \quad , \quad T_i = b\Omega_i^2 \quad (8)$$

So we have:

$$\vec{M} = \begin{bmatrix} \tau_x \\ \tau_y \\ \tau_z \end{bmatrix} = \begin{bmatrix} -(T_2 - T_4).L \\ (T_1 - T_3).L \\ (-\tau_1 - \tau_3 + \tau_2 + \tau_4) \end{bmatrix} = \begin{bmatrix} -(T_2 - T_4).L \\ (T_1 - T_3).L \\ \frac{d}{b}(T_2 + T_4 - T_1 - T_3) \end{bmatrix} \quad (9)$$

In the above equation, τ_x, τ_y and τ_z are roll, pitch and yaw torques respectively. L is the distance between the center of body mass and the axis of propeller rotation. Using equations (7) and (9) and rewriting the obtained equation in terms of the derivatives of angular velocities, we have:

$$\begin{bmatrix} \dot{\omega}_x \\ \dot{\omega}_y \\ \dot{\omega}_z \end{bmatrix} = \begin{bmatrix} \frac{\tau_x}{I_x} - \omega_y\omega_z\frac{(I_z - I_y)}{I_x} - \frac{J_r\Omega\omega_y}{I_x} \\ \frac{\tau_y}{I_y} - \omega_x\omega_z\frac{(I_x - I_z)}{I_y} + \frac{J_r\Omega\omega_x}{I_y} \\ \frac{\tau_z}{I_z} - \omega_x\omega_y\frac{(I_y - I_x)}{I_z} \end{bmatrix} \quad (10)$$

Now it is obligatory to obtain a relation between angular velocities about body axes and rates of Euler angles. To achieve this, the rates are transferred to the body coordinate system and by assuming small Euler angles finally we will have:

$$\begin{bmatrix} \omega_x \\ \omega_y \\ \omega_z \end{bmatrix} = \begin{bmatrix} \dot{\phi} - \sin(\theta)\dot{\psi} \\ \cos(\phi)\dot{\theta} + \sin(\phi)\cos(\theta)\dot{\psi} \\ -\sin(\phi)\dot{\theta} + \cos(\phi)\cos(\theta)\dot{\psi} \end{bmatrix} \quad (11)$$

Using above equation and equation (10), and neglecting terms consisting 3 and 4 terms products and presenting in terms of Euler angles we will have:

$$\begin{bmatrix} \ddot{\phi} \\ \ddot{\theta} \\ \ddot{\psi} \end{bmatrix} = \begin{bmatrix} a_1.(\dot{\theta}\dot{\psi}) - a_4.(\dot{\theta} + \phi\dot{\psi}).\Omega + b_3\tau_z\theta + b_1\tau_x \\ a_2.(\dot{\phi}\dot{\psi}) + a_5.(\dot{\phi} - \theta\dot{\psi}).\Omega - b_3\tau_z\phi + b_2\tau_y \\ a_3.(\phi\dot{\theta}) + (a_5\Omega\dot{\phi} + b_2\tau_y).\phi + b_3\tau_z \end{bmatrix} \quad (12)$$

Where:

$$\begin{aligned} a_1 &= \left[\frac{(I_y - I_z)}{I_x} + 1\right] \quad , \quad a_2 = \left[\frac{(I_z - I_x)}{I_y} - 1\right] \\ a_3 &= \left[\frac{(I_x - I_y)}{I_z} + 1\right] \quad , \quad a_4 = \frac{J_r}{I_x} \\ a_5 &= \frac{J_r}{I_y} \quad , \quad b_1 = \frac{1}{I_x} \quad , \quad b_2 = \frac{1}{I_y} \quad , \quad b_3 = \frac{1}{I_z} \end{aligned} \quad (13)$$

Finally to study the system we consider:

$$\begin{cases} x_1(t) = \phi(t) \\ x_2(t) = \dot{\phi}(t) \\ x_3(t) = \theta(t) \\ x_4(t) = \dot{\theta}(t) \\ x_5(t) = \psi(t) \\ x_6(t) = \dot{\psi}(t) \end{cases} \quad , \quad \begin{cases} U_2(t) = \tau_x \\ U_3(t) = \tau_y \\ U_4(t) = \tau_z \\ \delta = \Omega \end{cases} \quad (14)$$

So rewriting equations (12) and (13) using state space notation, we have:

$$\begin{cases} \dot{x}_1 = x_2 \\ \dot{x}_2 = a_1.(x_4.x_6) - a_4.(x_4 + x_1.x_6).\Omega + \\ \quad + b_3.u_4.x_3 + b_1.u_2 \\ \dot{x}_3 = x_4 \\ \dot{x}_4 = a_2.(x_2.x_6) + a_5.(x_2 - x_3.x_6).\Omega - \\ \quad - b_3.u_4.x_1 + b_2.u_3 \\ \dot{x}_5 = x_6 \\ \dot{x}_6 = a_3.(x_2.x_4) + a_5.(x_1.x_2).\Omega + \\ \quad + b_2.u_3.x_1 + b_3.u_4 \end{cases} \quad (15)$$

4 PHYSICAL PARAMETERS OF THE QUADROTOR

Table 1 presents the physical parameters of AR. Drone needed for simulation that have been measured.

Symbol	Definition	Value	Unit
m	Quadrotor mass	335	gr
L	Arm length	18	Cm
I_z	Moment of inertia about z axis	4.7×10^{-3}	Kg.m^2
I_x	Moment of inertia about x axis	1.8×10^{-3}	Kg.m^2
I_y	Moment of inertia about z axis	1.8×10^{-3}	Kg.m^2
b	Propeller Thrust factor	5.7231×10^{-6}	N.s^2
d	Propeller Drag factor	1.7169×10^{-7}	N.m.s^2
J_r	Rotor inertia	1.85×10^{-5}	Kg.m^2

Table 1: Physical parameters of the quadrotor.

Moment of Inertia: There is a common method to measure moment of inertia. This method is to make body oscillate. In this method, by measuring the period of the oscillating body, the moment of inertia about different axis is obtained.

Propeller thrust factor: Thrust is measured for different values of *n* and thrust in terms of *n* is estimated as follows:

$$\begin{aligned} &T = a_1 n^2 + a_2 n + a_3 \quad (5 \le n \le 500) \\ &a_1 = 3 \times 10^{-6} \, , \, a_2 = 0.001 \, , \, a_3 = 0.0907 \end{aligned} \quad (16)$$

http://www.imavs.org/

Combining (3) and (16) we have:

$$T = 5.7231 \times 10^{-6}\omega_p^2 \tag{17}$$

Then we have:

$$b = 5.7231 \times 10^{-6} \tag{18}$$

Propeller Drag factor: Produced moment is measured for different values of *n* and similar to the previous section, we will have:

$$d = 1.7169 \times 10^{-7} \tag{19}$$

5 ROTATIONAL CONTROL OF THE CONSTRAINED QUADROTOR

Quadrotor is a 6 DOF system and so it is an underactuated system but our aim is to control quadrotor rotations. The system is 3DOF and so it is an overactuated system. To study an overactuated system, it is possible to optimize a cost function which is U_1in this study, U_1 is total thrust:

$$U_1 = T_1 + T_2 + T_3 + T_4 \tag{20}$$

The optimal value for U_1 is the least possible value to keep motors running. Using equations (9), (14) and (20) we have:

$$T_1 = \tfrac{1}{4}U_1 + \tfrac{1}{2l}U_3 - \tfrac{b}{4d}U_4 \quad , \quad T_2 = \tfrac{1}{4}U_1 - \tfrac{1}{2l}U_2 + \tfrac{b}{4d}U_4$$

$$T_3 = \tfrac{1}{4}U_1 - \tfrac{1}{2l}U_3 - \tfrac{b}{4d}U_4 \quad , \quad T_4 = \tfrac{1}{4}U_1 + \tfrac{1}{2l}U_2 + \tfrac{b}{4d}U_4$$

$$\Rightarrow \begin{bmatrix} T_1 \\ T_2 \\ T_3 \\ T \end{bmatrix} = \begin{bmatrix} 1 & 1 & 1 & 1 \\ 0 & -l & 0 & l \\ l & 0 & -l & 0 \\ -\frac{d}{b} & \frac{d}{b} & -\frac{d}{b} & \frac{d}{b} \end{bmatrix} \begin{bmatrix} U_1 \\ U_2 \\ U_3 \\ U_4 \end{bmatrix} \tag{21}$$

In the following section, total thrust will be optimized using equations in (21).

5.1 Optimization of total thrust

Let's look at equations in (21). As it is observed each of T_1, T_2, T_3 and T_4 consists of 3 terms, a common $^1/_4U_1$ and two other terms, which are named $\bar{U}_i$ $(i = 1,\ 2,\ 3,\ 4)$:

$$\begin{aligned} \bar{U}_1 &= +\tfrac{1}{2l}U_3 - \tfrac{b}{4d}U_4 \quad , \quad \bar{U}_2 = -\tfrac{1}{2l}U_2 + \tfrac{b}{4d}U_4 \\ \bar{U}_3 &= -\tfrac{1}{2l}U_3 - \tfrac{b}{4d}U_4 \quad , \quad \bar{U}_4 = +\tfrac{1}{2l}U_2 + \tfrac{b}{4d}U_4 \end{aligned} \tag{22}$$

Now, one can prove that all values of $\bar{U}_i$ can not be positive values simultaneously. Let's assume all values for $\bar{U}_i$ are positive: $\bar{U}_i > 0$ Then simply we will have:

$$\begin{aligned} \bar{U}_1 > 0 \ , \ \bar{U}_2 > 0 \quad &\Rightarrow \ \mathrm{U}_2 < U_3 \\ \bar{U}_3 > 0 \ , \ \bar{U}_4 > 0 \quad &\Rightarrow \ \mathrm{U}_3 < U_2 \end{aligned}$$

So it is clear that at least for one $\bar{U}_i$ we have: $\bar{U}_i < 0$ Now, considering the mentioned point we can determine min(U_1) as follows:

$$U_1 = 4\left|\min \bar{U}_i\right| + T_{\min} \tag{23}$$

$T_{\min}$is the minimum thrust that can be obtained by replacing *n=5* into equation (16):

$$T_{\min} = 0.096N$$

5.2 Propeller-motor model

Combining equations (3) and (17), we will have:

$$n = 1.3812\sqrt{\frac{T}{5.7231 \times 10^{-6}}} - 173.895 \tag{24}$$

This equation gives required value of *n* to control the quadrotor.

5.3 PID Controller

The output of a PID controller, is the control input to the system and in the time-domain it is as follows:

$$U = K_P e + K_d\frac{de}{dt} + K_i\int edt \tag{25}$$

Where e is the error signal. Then for Euler angles we will have:

$$\begin{aligned} U_2(t) &= k_{p\phi}(\phi_d - \phi) + k_{d\phi}(\dot{\phi}_d - \dot{\phi}) + k_{i\phi}\textstyle\int(\phi_d - \phi)dt \\ U_3(t) &= k_{p\theta}(\theta_d - \theta) + k_{d\theta}(\dot{\theta}_d - \dot{\theta}) + k_{i\theta}\textstyle\int(\theta_d - \theta)dt \\ U_4(t) &= k_{p\psi}(\psi_d - \psi) + k_{d\psi}(\dot{\psi}_d - \dot{\psi}) + k_{i\psi}\textstyle\int(\psi_d - \psi)dt \end{aligned} \tag{26}$$

PID controller coefficients are given in Table 2. Both theorical and experimental coefficients have been obtained by try and error.

	Coefficient	Theorical	Experimental
Roll Control	$k_{p\phi}$	0.08	0.1
	$k_{d\phi}$	0.02	0.05
	$k_{i\phi}$	0.09	0.06
Pitch Control	$k_{p\theta}$	0.08	0.1
	$k_{d\theta}$	0.03	0.0.5
	$k_{i\theta}$	0.07	0.06
Yaw Control	$k_{p\psi}$	0.07	0.09
	$k_{d\psi}$	0.03	0.05
	$k_{i\psi}$	0.09	0.05

Table 2: PID Coefficients.

5.4 Backstepping Controller

Backstepping method is presented in [16] completely and we briefly explain it then we will use it for the quadrotor. We consider the special case of integrator backstepping. Consider the system:

$$\begin{aligned} \dot{\eta} &= f(\eta) + G(\eta)\zeta \\ \dot{\zeta} &= f_a(\eta,\zeta) + G_a(\eta,\zeta)u \end{aligned} \tag{27}$$

Where $f_a$and $G_a$are smooth. The state-space equation (15) is considered and vector of variables and input are defined as following:

$$\eta = \begin{bmatrix} x_1 \\ x_3 \\ x_5 \end{bmatrix} \ , \ \zeta = \begin{bmatrix} x_2 \\ x_4 \\ x_6 \end{bmatrix} \ , u = \begin{bmatrix} U_2 \\ U_3 \\ U_4 \end{bmatrix} \tag{28}$$

http://www.imavs.org/

Backstepping controller design is a two-step method. In first step, it is assumed that ζ is the input of the first equation of equations (27). The first equation is stabilized using $\zeta = \Phi(\eta)$ in a way that it will be possible to find a Lyapunov function for the first equation. $\Phi(\eta)$ is considered as following:

$$\Phi(\eta) = \begin{bmatrix} -k_1 & 0 & 0 \\ 0 & -k_3 & 0 \\ 0 & 0 & -k_5 \end{bmatrix} \begin{bmatrix} x_1 \\ x_3 \\ x_5 \end{bmatrix} = \begin{bmatrix} -k_1 x_1 \\ -k_3 x_3 \\ -k_5 x_5 \end{bmatrix}$$
$$k_1 \ , k_3 \ , \ k_5 \ > \ 0 \tag{29}$$

In this step, Lyapunov function $V(\eta)$ is considered as following:

$$V(\eta) = \frac{1}{2}\eta^T \eta = \frac{1}{2}(x_1^2 + x_3^2 + x_5^2) \tag{30}$$

In second step, for Lyapunov function, V_a, we consider:

$$V_a = V(\eta) + \frac{1}{2}\left[\zeta - \Phi(\eta)\right]^T \left[\zeta - \Phi(\eta)\right] \tag{31}$$

Now *u* is considered such that the derivative of the Lyapunov function to be negative and to stabilize the second equation. Considering *u* as following:

$$u = G_a^{-1}\left[\frac{\partial \Phi}{\partial \eta}(f + G\zeta) - (\frac{\partial V}{\partial \eta}G)^T - f_a - K(\zeta - \Phi)\right] \tag{32}$$

Where:

$$K = \begin{bmatrix} k_2 & 0 & 0 \\ 0 & k_4 & 0 \\ 0 & 0 & k_6 \end{bmatrix}$$
$$k_2 \ , k_4 \ , k_6 > \ 0 \tag{33}$$

And substituting related functions in (32) we have:

$$u = \begin{bmatrix} b_1 & 0 & b_3 x_3 \\ 0 & b_2 & -b_3 x_1 \\ 0 & b_2 x_1 & b_3 \end{bmatrix}^{-1} \begin{bmatrix} (-k_1 x_2 - k_2 x_2 - k_1 k_2 x_1 - \\ x_1 - a_1 x_4 x_6 + \\ a_4.(x_4 + x_1 x_6).\Omega_r) \\ \\ (-k_3 x_4 - k_4 x_4 - k_3 k_4 x_3 - \\ x_3 - a_2 x_2 x_6 - \\ a_5.(x_2 - x_3 x_6).\Omega_r) \\ \\ (-k_5 x_6 - k_6 x_6 - k_5 k_6 x_5 - \\ x_5 - a_3 x_2 x_4 \\ -a_5 x_1 x_2.\Omega_r) \end{bmatrix} \tag{34}$$

To implement Backstepping controller on real model, let's assume that ω_x, ω_y and ω_z are equal to $\dot{\varphi}$, $\dot{\psi}$ and $\dot{\theta}$. If Euler angles are small, this assumption will be valid. So, equation (15) will change to the following equations in state-space form:

$$\begin{cases} \dot{x}_1 = x_2 \\ \dot{x}_2 = a_1.(x_4.x_6) - a_4.x_4.\Omega + b_1.U_2 \\ \dot{x}_3 = x_4 \\ \dot{x}_4 = a_2.(x_2.x_6) + a_5.x_2.\Omega + b_2.U_3 \\ \dot{x}_5 = x_6 \\ \dot{x}_6 = a_3.(x_2.x_4) + b_3.U_4 \end{cases} \tag{35}$$

Where:

$$\begin{array}{lll} a_1 = \frac{(I_y - I_z)}{I_x} & , & a_2 = \frac{(I_z - I_x)}{I_y} \\ a_3 = \frac{(I_x - I_y)}{I_z} & , & a_4 = \frac{J_r}{I_x} \\ a_5 = \frac{J_r}{I_y} & & \end{array} \tag{36}$$

Similar to the previous state:

$$u = \begin{bmatrix} \frac{1}{b_1} & 0 & 0 \\ 0 & \frac{1}{b_2} & 0 \\ 0 & 0 & \frac{1}{b_3} \end{bmatrix} \begin{bmatrix} (-k_1 x_2 - k_2 x_2 - k_1 k_2 x_1 - \\ x_1 - a_1 x_4 x_6 + a_4.x_4.\Omega_r) \\ \\ (-k_3 x_4 - k_4 x_4 - k_3 k_4 x_3 - \\ x_3 - a_2 x_2 x_6 - a_5.x_2.\Omega_r) \\ \\ (-k_5 x_6 - k_6 x_6 - k_5 k_6 x_5 - \\ x_5 - a_3 x_2 x_4) \end{bmatrix} \tag{37}$$

Equation (34) is used in simulation and equation (37) is used in the experimental method. values of *ki , i=1 to 6*, are obtained using try and error in both simulation and experimental method. These coefficients are given in Table 3.

Parameters	Simulation	Experimental
$\mathbf{k}_1$	14	10
$\mathbf{k}_2$	5	3
$\mathbf{k}_3$	10	10
$\mathbf{k}_4$	5	3
$\mathbf{k}_5$	10	6
$\mathbf{k}_6$	4	2

Table 3: Backstepping Coefficients.

6 SIMULATION RESULTS

In the following figures, Euler angles controlled by PID and backstepping controllers are shown.

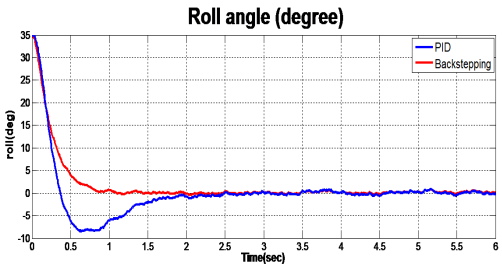

Figure 6: Roll controlled by PID and Backstepping

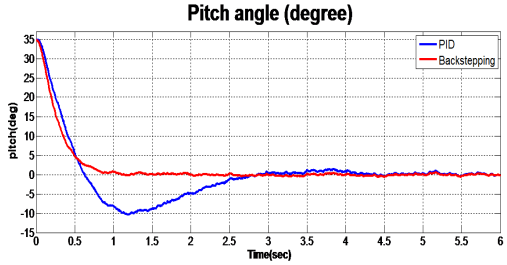

Figure 7: Pitch controlled by PID and Backstepping

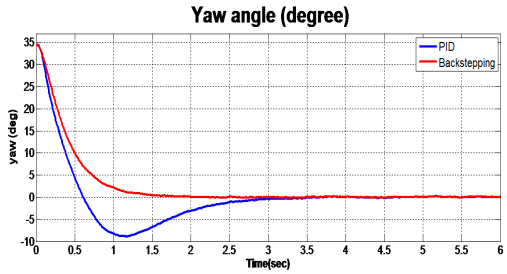

Figure 8: Yaw controlled by PID and Backstepping

As it is seen in the above figures backstepping controller has regulated angles to zero about 1.5 to 2 seconds faster than PID controller. Following figures indicate the input signals to the motors and as it is seen maximum values for n in PID is more than in backstepping.

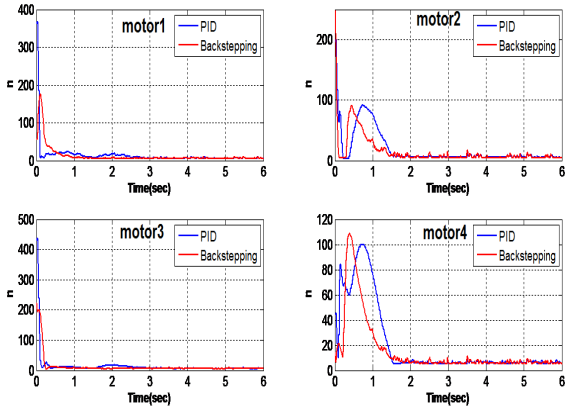

Figure 9: The input signals to the motors in PID and Backstepping Controllers

7 EXPERIMENTAL RESULTS FOR PID AND BACKSTEPPING

Following figures indicate experimental results for PID and Backstepping controllers. In each figure, one channel has been excited by tapping. As it is seen in experimental results, by exciting one channel the other channels are excited too.

PID:

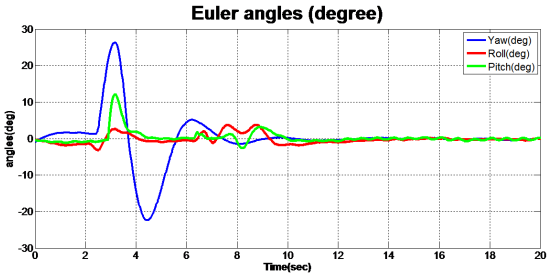

Figure 10: The Euler angles controlled by PID when Yaw is excited

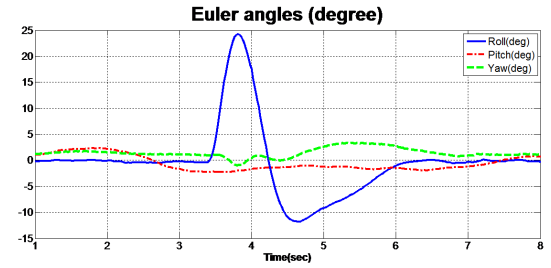

Figure 11: The Euler angles controlled by PID when Roll is excited

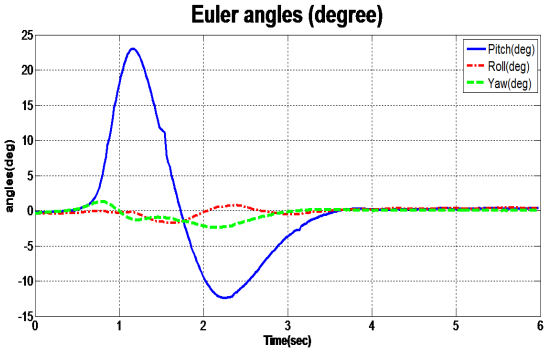

Figure 12: The Euler angles controlled by PID when Pitch is excited

Backstepping:

http://www.imavs.org/

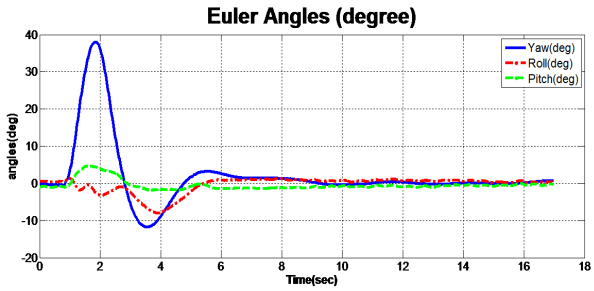

Figure 13: The Euler angles controlled by Backstepping when Yaw is excited

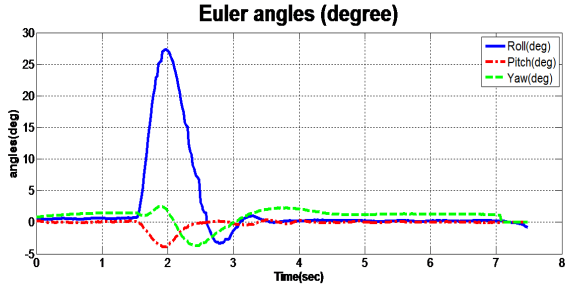

Figure 14: The Euler angles controlled by Backstepping when Roll is excited

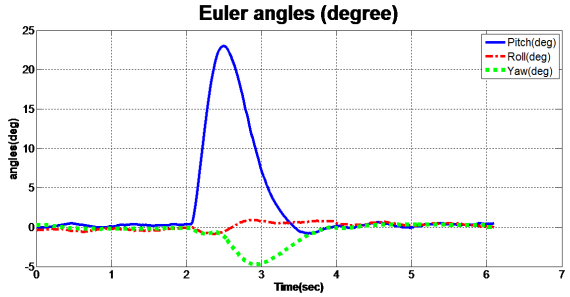

Figure 15: The Euler angles controlled by Backstepping when Pitch is excited

In Figures 12 and 15, Pitch is excited 23 degrees, as it is seen it has taken about 2 seconds in backstepping to regulate but it is about 2.7 seconds in PID. In two other angles Backstepping has controlled bigger disturbances in shorter time and this shows Backstepping acted faster than PID.

8 CONCLUSION

Rotational model of the quadrotor was simulated and some physical parameters are measured by methods that are explained briefly. Then backstepping controller was implemented on simulated model and the results were compared with those of PID. Then both control methods were implemented on real model. Results have shown that Backstepping acted faster than PID. However PID was easier to implement to control without having full information of the plant.

REFERENCES

[1] S. Bouabdallah, P. Murrieri, and R. Siegwart, "Design and Control of an Indoor Micro Quadrotor," *IEEE Int. Conf. Robot. Autom.* 2004. Proceedings. ICRA '04. 2004, vol. 5, April, 2004.

[2] P. Castillo, a Dzul, and R. Lozano, "Real-time Stabilisation and Tracking of a Four Rotor Mini-rotorcraft" *IEEE Trans. Control Syst. Technol.*, 2004.

[3] A. Tayebi and S. McGilvray, "Attitude Stabilization of a VTOL Quadrotor Aircraft," *IEEE Trans. Control Syst. Technol.*, vol. 14, no. 3, 2006.

[4] Y. Morel and A. Leonessa, "Direct Adaptive Tracking Control of Quadrotor Aerial Vehicles," *Dyn. Syst. Control. Parts A B*, 2006.

[5] A. O. Kivrak, "Design of Control Systems for a Quadrotor," A Master's Thesis in Mechatronics Engineering, Atilim University, December, 2006.

[6] G. Hoffmann, D. G. Rajnarayan, S. L. Waslander, D. Dostal, M. Candidate, J. S. Jang, and C. J. Tomlin, "The Stanford Testbed of Autonomous Rotorcraft For Multi Agent Control System Hardware Full System,", Stanford University, 2004.

[7] T. Madani and A. Benallegue, "Backstepping Control for a Quadrotor Helicopter," *2006 IEEE/RSJ Int. Conf. Intell. Robot. Syst.*, 2006.

[8] A. Soumelidis, P. Gspr, G. Regula, and B. Lantos, "Control of an Experimental Mini Quad-rotor UAV," *2008 Mediterr. Conf. Control Autom. - Conf. Proceedings, MED'08*, 2008.

[9] M. Guisser and H. Medromi, "A High Gain Observer and Sliding Mode Controller for an Autonomous Quadrotor Helicopter," *Int. J. Intell. Control Syst.*, vol. 14, 2009.

[10] A. Mokhtari and A. Benallegue, "Dynamic Feedback Controller of Euler Angles and Wind Parameters Estimation for a Quadrotor Unmanned Aerial Vehicle," *IEEE Int. Conf. Robot. Autom. 2004. Proceedings. ICRA '04*. 2004, vol. 3, 2004.

[11] N. Guenard, T. Hamel, and R. Mahony, "A Practical Visual Servo Control for an Unmanned Aerial Vehicle," vol. 24, no. 2, 2008.

[12] H. Voos, "Nonlinear and Neural Network-based Control of a Small Four-Rotor Aerial Robot," *Int. Conf. Adv. Intell. mechatronics*, 2007.

[13] N. Dijkshoorn, "Simultaneous Localization and Mapping with the AR . Drone," , *Master's Thesis in Artifial Intelligence, Univ. Van Amsterdam*, 2012.

[14] A. Naghash, M. Naghshineh, and A. Honari, "Minimum Time Trajectory Optimization for Flying a Quadrotor in an 8 - shaped Path," , *International Micro Air Vehicle Conference*, September, 2013.

[15] S. N. Ghazbi, A. L. I. Akbar, and M. Reza, "Quadrotor: Full Dynamic Modeling , Nonlinear Simulation and Control of Attitudes Degrees of Freedom and the Movement," vol. 1,

http://www.imavs.org/

no. 2, 2014.
[16] H. Khalil, "Nonlinear Systems.", Prentice Hall, 2002.

http://www.imavs.org/